THE ASTROPHYSICAL JOURNAL SUPPLEMENT SERIES, 97:331–346, 1995 April

ULTRAVIOLET TO OPTICAL SPECTRAL DISTRIBUTIONS OF NORTHERN STAR-FORMING GALAXIES

KERRY MCQUADE, DANIELA CALZETTI,[1] AND ANNE L. KINNEY[1]
Space Telescope Science Institute, 3700 San Martin Drive, Baltimore MD 21218
Received 1994 July 18; accepted 1994 September 22

ABSTRACT

We report spectral energy distribution from the UV to the optical for a sample of 31 northern star-forming galaxies. We also present measurements for emission-line fluxes, continuum levels, and equivalent widths of absorption features for each individual spectrum as well as averages for the eight galactic activity classes, including normal, starburst, Seyfert 2, blue compact dwarf, blue compact, LINER, H II, and combination LINER–H II galaxies.

Subject headings: galaxies: starbursts — galaxies: stellar content — stars: formation — ultraviolet: galaxies

1. INTRODUCTION

A comparison of spectral properties of high-redshift galaxies with nearby galaxies requires that the nearby galaxies be observed in a large aperture so that their spectra are integrated over the disk of the galaxy. Such a method was used by Kennicutt (1992a, b) in the optical from 3650 to 7100 Å with 5 to 8 Å resolution. We extend the Kennicutt method by combining the UV spectra of star forming galaxies from Kinney et al. (1993) with optical spectra in an aperture matched to the size of the *IUE* aperture, resulting in integrated spectra in the range from 1200 to 7800 Å with spectral resolution of 5 to 10 Å. We report the spectral energy distributions of 31 galaxies observed at KPNO. Our targets are complementary to the 49 southern galaxies observed at CTIO and reported by Storchi-Bergmann, Kinney, & Challis (1995). The basic properties of the galaxies can be found in Table 1 of Kinney et al. (1993).

2. OBSERVATIONS

The spectra were observed in 1991 September and 1992 July at KPNO with the 0.9 m and the Intensified Reticon Scanner (IRS), using a circular aperture of 13″.5 diameter, which matches the large (10″ × 20″) *IUE* aperture closely in area. Because of the close match in optical/UV aperture size, no normalization was necessary between the two wavebands. The number 26 grating and the number 35 grating were used to achieve coverage in the wavelength region from 3500 Å to 8000 Å with 10 Å resolution. Table 1 presents a log of the observations.

The spectra were flat-fielded, wavelength calibrated, flux calibrated, and corrected for atmospheric extinction using standard IRAF packages. The spectra have also been corrected for extinction induced by the eruption from Mount Pinatubo (NOAO Newsletter, 1991 December). They have not, however, been corrected for Galactic extinction. In all but one spectrum, NGC 1569 [$E(B-V) = 0.51$], this effect is negligible.

[1] Visiting Astronomer, Kitt Peak National Observatory, National Optical Astronomy Observatories, which is operated by AURA, Inc., under a cooperative agreement with the National Science Foundation.

3. ANALYSIS

Prior to analysis, all the spectra were brought back to the rest frame. Redshifts were calculated from the recessional velocities given in Table 1 of Kinney et al. (1993).

In order to derive a continuum from which to measure the absorption features, we measure the flux values at 18 wavelengths, which were selected because they were free from the emission-line features listed in Table 2 and the absorption-line features listed in Table 3. For the UV wavelength selection, we chose those continuum regions used in Robert, Leitherer, & Heckman (1993); the optical continuum regions were chosen from Bica (1988). The continuum flux was calculated as the 1σ–clipped median value of a 60 Å wide bin centered on each wavelength point. This is a larger bin size than that of Storchi-Bergmann, Kinney, & Challis (1995), necessitated by the low signal-to-noise ratio of our spectra in comparison to theirs. All fluxes were then inspected visually to eliminate skewed values caused by noise or other features. For example, the flux at λ6563 is usually located in the Hα emission line, so the measurement here was taken as a visual estimate at the base of the feature, usually around λ6520. The specific continuum wavelengths and corresponding fluxes are shown in Table 4. Those fluxes that were determined by a visual estimate are marked with an asterisk.

Equivalent widths for the absorption features listed in Table 3 were measured and are reported in Table 5. To ensure consistency, the features were measured between the same wavelengths for all spectra. We have chosen an equivalent width of 1 Å as the lower limit of a true detection. Equivalent widths of less than 1 Å indicate that the spectrum is too noisy for an accurate measurement, or that the data contain a dropout in the region of the feature. Features located in noisy portions of the spectrum (all the UV features and the TiO features) have errors of up to 50%. Otherwise, the error is generally around 10%–15%.

The emission lines listed in Table 2 have been separated into two groups. The most commonly found emission lines are measured in Table 6, while the UV and less common lines are measured in Table 7. As in Table 5, lines with uncertainties of 50% are marked with a colon.

TABLE 1

OBSERVATION LOG

GALAXY	DIAMETER	DATE	EXPOSURE TIME (s) 3200–6000 Å	5000–8000 Å
NGC 224	190′ × 60′	1991 Sep	240	280
IC 1586	0.3 × 0.3	1991 Sep	3600	4000
NGC 262	1.1 × 1.1	1991 Sep	4240	4640
Mrk 357	0.2 × 0.2	1991 Sep	7200	2680
NGC 598	70.8 × 41.7	1991 Sep	1200	1400
IC 214	0.5 × 0.7	1991 Sep	4320	4320
NGC 1023	8.7 × 3.0	1991 Sep	600	800
NGC 1068	7.1 × 6.0	1991 Sep	320	400
NGC 1569	3.6 × 1.8	1991 Sep	600	800
NGC 1614	1.3 × 1.1	1991 Sep	6000	1800
NGC 1667	1.8 × 1.4	1991 Sep	3240	1800
NGC 2403	21.9 × 12.3	1991 Sep	1200	1520
NGC 3031	26.9 × 14.1	1991 Sep	800	240
NGC 3077	5.4 × 4.5	1991 Sep	1200	1200
NGC 4194	1.8 × 1.1	1992 Jul	1800	1800
NGC 4853	0.8 × 0.8	1992 Jul	1200	2400
NGC 4861	4.0 × 1.5	1992 Jul	...	1200
Mrk 66	0.4 × 0.3	1992 Jul	2400	2400
Mrk 477	...	1992 Jul	1200	1800
NGC 5728	3.1 × 1.8	1992 Jul	1000	1000
UGC 9560	0.7 × 0.3	1992 Jul	1200	1800
NGC 5860	0.5 × 0.6	1992 Jul	2400	2400
UGCA 410	0.3 × 0.2	1992 Jul	2400	4800
NGC 5996	1.7 × 0.9	1992 Jul	1200	1200
NGC 6052	1.0 × 0.7	1992 Jul	1200	1200
NGC 6090	0.6 × 0.6	1991 Sep	2040	3600
NGC 6217	3.0 × 2.5	1991 Sep	3600	920
Mrk 499	0.2 × 0.2	1991 Sep	3600	2400
NGC 6764	2.3 × 1.3	1991 Sep	1600	1800
NGC 7250	1.7 × 0.8	1991 Sep	2160	2200
Mrk 309	0.5 × 0.3	1991 Sep	4240	4640
NGC 7673	1.3 × 1.2	1991 Sep	3720	2400
NGC 7714	1.9 × 1.4	1991 Sep	1760	2000
Mrk 542	0.2 × 0.2	1992 Jul	5400	4200

4. DIGITAL DISTRIBUTION OF THE DATA

Files containing the spectra will be available in digital form through the National Space Science Data Center (NSSDC) and, for a limited time via anonymous ftp at node ftp.stsci.edu. The files will be available in both FITS format and in ASCII. The data will be available via nssdc.gsfc.nasa.gov. Electronic mail requests can be directed to archives@ndadsa.gsfc.nasa.gov. The node ftp.stsci.edu (130.167.1.2) will contain the data in the directory observer/catalogs.

5. DISCUSSION

Figures 1–8 contain sample UV + optical spectra from each classification group. Our sample contains normal, starburst (SB), Seyfert 2 (Sy2), blue compact dwarf (BCDG), blue compact (BCG), LINER (Lin), H II, and composite LINER–H II (Lin-HII) galaxies. These are the classifications presented in Kinney et al. (1993). We differ only in the classification of NGC 4853, which is listed in Kinney et al. (1993) as a BCDG. We classify it as a normal galaxy.

In the sample plots, the bar across the top of the spectrum marks emission lines at the galaxy's redshift. The bar beneath the spectrum corresponds to common absorption features.

TABLE 2

EMISSION LINES

Line	Rest Wavelength (Å)
Lyα	1216
C IV	1548, 1550
He II	1640
C III]	1908
C II]	2326
[Ne IV]	2424
Mg II	2796, 2803
[Ne V]	3426
[O II]	3726, 3729
[Ne III]	3869
Hγ	4340
[O III]	4363
He II	4686
Hβ	4861
[O III]	5007
He I	5876
[O I]	6300
Hα	6563
[N II]	6584
[S II]	6717
[S II]	6731
[Ar III]	7135
[O II]	7319, 7330

The rest wavelengths of the emission lines and absorption features are found in Tables 2 and 3, respectively.

5.1. *Comparison with Previous Work by Kennicutt (1992b)*

Our sample of Northern galaxies contains 10 galaxies which appear in the analysis of Kennicutt (1992b): NGC 1569, NGC 3077, NGC 4194, NGC 4861, UGCA 410, NGC 5996, NGC 6052, NGC 6217, NGC 6764, and NGC 7714. Eight of the 10 galaxies show remarkable resemblance in the shape of the continuum and in the emission-line strengths and emission-line ratios.

Our spectrum of NGC 1569 shows a bluer optical spectrum here (Fig. 2) than in Kennicutt (1992b, Fig. 18). The aperture used by Kennicutt is much larger than ours (45″ circular versus 13″.5 circular). Since NGC 1569 has a very large radius of 1′48″

TABLE 3

ABSORPTION FEATURES

Identification	Window (Å)
Si IV	1380–1415
C IV	1523–1576
Fe II	2570–2615
Mg II	2780–2825
Ca K	3908–3952
Ca H	3952–3988
CN	4150–4214
G band	4284–4318
Mg	5156–5196
Na I	5880–5914
TiO	6156–6274
TiO	7158–7274

TABLE 4

FLUXES AT SELECTED CONTINUUM WAVELENGTHS

GALAXY	1355	1455	1507	1583	2330	2900	3500	3740	3810	4020	4510	4630	5312	5870	6080	6563	7043	7525
NGC224	8.6	8.6	7.6	6.8*	5.2*	20.1*	59.7	63.9	60.2*	138.2	231.1*	247.6	295.4	293.2	338.0	330.0*	347.7	395.1
IC1586	5.6	5.6	5.6	4.4	—	—	3.5	3.7*	3.5*	4.3*	4.4	4.4*	3.9	3.6	3.5	3.3*	3.2	—
NGC262	1.6	1.4*	1.8	1.3*	—	—	2.2	1.9	2.2	2.0*	3.5	3.8*	4.3	4.9	5.1	4.8*	5.2	5.6*
MRK357	14.1	13.4	14.6	12.4	—	—	3.7	3.0*	3.1	3.1*	2.4	2.3*	1.9*	1.5	1.4	1.1*	1.6	—
NGC598	11.0*	10.4	11.1	8.7	8.1	9.5	10.8	11.5*	12.0*	14.4	15.0	14.7	13.7	13.5*	14.4	12.9*	12.6*	12.9
IC214	6.0	5.3	7.1	5.3	—	—	1.2	1.4	1.5*	2.1*	2.3	2.4	2.1	2.0*	2.2	2.4*	2.0*	—
NGC1023	—	—	—	—	1.3	4.4	13.2	17.2	15.5	33.1	56.2	62.1	72.7	79.8	82.4	79.7*	85.4	92.0
NGC1068	64.5	60.1	60.0*	58.1*	45.4	47.7	63.0	61.9*	64.6	85.7*	111.0	115.2	119.7*	119.0	121.6*	110.4*	106.6	106.6
NGC1569	6.1	10.6	11.6	10.5	10.7	15.7	18.7	18.5*	20.6*	20.6	20.5	20.6	21.7	20.8	21.5	20.0*	20.9*	22.6
NGC1614	4.5	5.2	5.5	4.1	—	—	3.4	3.7	3.5*	4.6*	5.3	5.4	5.9	7.0	7.7	7.6*	8.1	—
NGC1677	2.9	1.8	2.7	1.6	—	—	2.6*	3.4	3.8*	4.4*	6.9	7.4	7.6	9.1*	9.5	9.3*	10.6*	9.8
NGC2403	2.7	2.8	5.2	2.9	1.7	2.7	2.2*	2.2*	1.8	1.7	1.4	1.4*	0.9*	0.7*	0.7*	0.4*	0.5	0.4
NGC3031	2.7	1.9	3.9	2.8	3.1*	9.8	32.0*	42.1*	36.5*	73.5*	126.8	134.5	163.4	185.9*	199.8*	201.2*	202.3	220.7
NGC3077	9.8	8.9	8.3	8.3	—	—	—	5.6*	9.3	13.6	13.4	14.1	12.6	11.5	12.5*	11.7*	10.9	11.8
NGC4194	14.7	14.4	15.2	14.2	14.1	13.5	12.7	12.6*	14.3	16.5	17.8	16.5	16.7	16.8*	17.2	17.0*	16.3	—
NGC4853	1.7	1.7	1.5	1.1	1.8	2.2	2.5	3.0	3.5	4.2	6.7	7.5	6.8	7.3*	7.5	7.1*	6.7*	—
NGC4861	115.2	101.0	95.3	80.6	25.5	19.3	—	—	—	—	—	—	3.1	2.9*	2.3*	2.4*	1.2	—
MRK66	10.7	10.6	11.2	8.6*	—	—	3.6	2.7	3.5*	3.9	3.7	3.7	2.8	2.3*	2.3*	2.0*	1.5	—
MRK477	6.8	6.7	6.8	5.5*	3.3*	2.9*	2.2	2.9	2.8	3.1*	3.0*	3.0	2.9	2.8	3.3	3.0*	2.5*	—
NGC5728	2.3	2.4	3.2	2.8	1.8	3.0	9.3	8.4	8.2	13.7	19.8	22.1	23.9	26.5	26.9	26.5*	27.7*	—
UGC9560	35.7	32.0	30.9*	24.9	10.2	7.6	5.0	3.6*	3.9*	4.0	3.3	3.2	2.6	2.6	2.2*	1.4*	1.8	—
NGC5860	7.2	5.9	7.6	6.1	4.0	4.3	4.2	4.6	5.2*	5.8*	7.0	7.4	6.6	6.6	6.7	6.4*	6.1	—
UGCA410	11.0	10.3	11.3	9.5	—	—	1.6	1.4*	1.6	1.5	1.5	1.4	1.3*	1.4*	1.3	1.0*	1.2	—
NGC5996	15.2	15.3	14.9	10.9	8.7	7.8	8.3	6.3	7.2	7.4	7.6	7.8	6.6	6.3	6.7	5.8*	6.1	—
NGC6052	11.7	12.6	13.4	10.2	8.5	7.5	7.3	8.2	9.1	9.4	9.7*	9.5*	8.6	7.9	7.6	7.0*	5.4	—
NGC6090	10.9*	10.5	12.0	7.2	—	—	5.0	4.2*	4.5*	6.0*	5.3	5.5	4.9*	5.3	5.1	4.8*	4.7	4.9
NGC6217	18.4	17.0	16.9	13.8	—	—	9.7	10.3*	11.4	13.4	13.2	13.2	12.3*	12.5	12.3	12.2*	13.2	13.5
MRK499	8.8*	9.5	10.6	8.2*	—	—	3.8*	3.1	3.4	4.2	4.1	4.1	3.4	3.1	3.1	2.7*	2.8	2.8
NGC6764	3.4	3.0	4.5	3.3	4.2	4.5	4.6	3.6*	4.4	4.4*	4.7	4.9	4.5*	4.7	4.8	4.9*	5.2	5.0
NGC7250	12.2	12.5	12.2	10.9	7.1	6.1	5.3	5.6*	5.7	6.2	5.9*	5.6	5.0*	4.8	4.6	4.1*	4.1	5.2
MRK309	1.3	1.7	2.1	2.8	—	—	2.7	2.5*	2.4*	2.7	2.7	2.7	2.2	1.9	2.0	1.8*	1.7*	—
NGC7673	22.8	22.4	22.5	17.3	10.1	8.7	9.2	8.6*	9.9	11.5	12.3	11.5	9.6	9.1	8.6	8.3*	7.8	8.3
NGC7714	37.4	36.5	37.2	30.9	19.9	18.2*	18.7	16.5*	18.4	20.2	19.6*	19.6	16.5	16.5	15.8	14.6*	15.0	14.6
MRK542	6.6	6.2	6.8	4.7	—	—	1.8	1.7	2.0*	2.7	2.9	3.0	2.7*	2.5	2.7	2.4*	2.6	—

NOTES.—Flux unit = 10^{-15} ergs s^{-1} cm^{-1} Å^{-1}. Median flux in 60 Å bin, with continuum points excluded when they deviate from the median value in the bin by more than 1 σ. Entries followed by an asterisk indicate that the measurement was a visual estimate.

TABLE 5

EQUIVALENT WIDTHS OF ABSORPTION FEATURES (Å)

Galaxy	SiIV	CIV	FeII	MgII	CaK	Ca	CN	G-band	Mg	NaI	TiO	TiO
NGC224	3.4:	2.6:	1.8	8.6	5.8	6.4	1.8	3.4	4.6	5.3	3.1	2.7
IC1586	6.0	8.0	—	—	2.4	5.7	1.0:	2.0	1.5:	2.7:	6.5:	—
NGC262	1.7:	—	—	—	6.1	2.5	—	6.6	3.8	1.3	0.8:	4.0
Mrk357	2.8	15.3	—	—	—	—	—	0.9:	1.5	—	15.7:	—
NGC598	3.8	4.6	3.0	6.7	5.3	1.3:	2.2	3.2	0.7:	1.0:	—	2.8:
IC214	7.8	7.7:	—	—	3.5:	6.8	3.8	2.4:	2.7:	2.8:	14.3:	—
NGC1023	—	—	0.8:	4.0	9.2	6.8	2.1	4.6	4.2	4.7	3.6	3.5:
NGC1068	—	—	1.4	—	9.8	—	1.2	3.9	1.6	1.5	1.2:	8.1:
NGC1569	2.4	5.7	3.0	4.6	1.6	0.6:	0.2:	1.6	1.1:	1.6	1.5:	7.6
NGC1614	8.0:	5.0:	—	—	1.9	1.9	—	—	1.4	3.2	0.2:	—
NGC1667	—	7.5:	—	—	3.6	5.6	3.1	3.3	2.4	1.3	2.7	10.4:
NGC2403	2.5:	6.2:	7.9	8.4	1.4	1.1:	0.9:	1.5:	3.8	—	0.1:	13.3:
NGC3031	—	—	2.0:	—	8.6	4.9	—	4.5	4.2	4.0	0.7:	6.6
NGC3077	3.7	—	—	—	2.4	4.7	—	—	0.5:	0.4:	—	2.8:
NGC4194	4.0	9.1	6.2	8.5	—	3.4	0.2:	0.7:	0.9:	1.3:	2.4	—
NGC4853	6.9:	19.2:	1.4:	1.2	3.0:	7.4	—	3.5	1.3	1.3	0.9:	—
NGC4861	2.3	3.8	1.3	—	—	—	—	—	—	0.4:	6.0:	—
Mrk66	3.4	5.4	—	—	0.4:	3.7	2.1	3.3	0.2:	3.4	—	—
Mrk477	—	—	6.3	—	3.6	—	1.4:	3.4	3.1	4.1	2.5:	—
NGC5728	0.8:	—	1.8:	—	8.9	2.6	4.1:	4.0	1.6:	2.7	0.2:	—
UGC9560	4.1	4.1	0.8:	3.2:	1.7:	—	—	1.8	—	1.1:	0.9:	16.8:
NGC5860	7.3	4.6:	5.0	7.6	1.2	6.5	—	0.6:	0.8:	1.6:	—	—
UGCA410	2.6:	1.3:	—	—	1.8	—	1.6:	7.1	0.8:	2.8	0.3:	68.3:
NGC5996	8.7	8.3	6.8	5.2	6.6	0.6:	3.3	2.2	2.3	0.6:	4.7	—
NGC6052	1.4	7.1	6.6	7.1	2.4:	2.5	—	0.2:	0.6:	1.1:	3.5:	—
NGC6090	1.6	9.0	—	—	3.8	0.6:	2.2:	0.2:	1.6	—	0.6:	2.5:
NGC6217	7.3	9.2	—	—	0.8:	3.6	0.3:	1.0	1.9	2.1	5.4:	3.7
Mrk499	5.3	9.6	—	—	—	4.9	0.8:	0.4:	1.4	1.6:	6.2:	—
NGC6764	8.7	5.7:	8.2:	6.3	7.7	5.9	0.4:	1.7	—	2.5	3.2:	2.0:
NGC7250	3.8	6.6	5.0:	2.0:	—	5.3	2.4	—	1.3	0.8:	2.2:	17.4:
Mrk309	14.3	—	—	—	2.8:	4.0	1.6:	—	1.4	2.1	2.2:	—
NGC7673	3.0	9.0	5.8	5.6	0.1:	3.4:	1.7:	1.3:	0.2:	0.1:	1.0:	—
NGC7714	5.2	7.6	4.4:	4.5:	0.8:	0.3:	0.4:	0.9:	1.0:	0.9:	0.6:	7.6:
Mrk542	6.5	9.2	—	—	1.3:	4.4	2.3	0.2:	0.7:	2.8:	3.2:	—

NOTE.—Entries followed by a colon indicate that the measurement has an error of >50% or that the feature identification is highly uncertain.

TABLE 6

FLUXES OF COMMON EMISSION LINES

Galaxy	[O II]	[Ne III]	Hg	[O III]	Hb	[O III]	He I	[O I]	Ha	[N II]	[S II]	[S II]
NGC224	—	—	—	—	—	—	—	—	—	67.9:	—	—
IC1586	138.8	18.5	8.6	1.7	38.8	52.3	7.0	—	229.3	48.1	48.0	26.4
NGC262	79.9	27.7	10.0	10.8	23.9	394.5	—	31.4	120.4	117.5	71.5	48.0
MRK357	127.0	11.9	28.0	5.3:	7.3	219.3	6.0	—	292.7:	51.7:	—	27.6
NGC598	237.9	—	25.8	—	34.9	51.8	—	—	—	—	—	—
IC214	35.9	2.9	5.4	3.5	21.4	39.0	—	—	152.2:	46.6:	39.3:	10.7:
NGC1068	2434.0	1454.4	655.0	329.9	1576.0	23065.7	131.4	904.8	19873.4	6196.9	2422.5:	—
NGC1569	279.0	81.2	84.4	—	253.2	1723.5	54.3	—	1852.1	—	103.3	92.9
NGC1614	95.2	—	19.8	7.9	92.0	77.4	10.6	13.1	1069.4	475.2	84.4	102.8
NGC1667	32.4	—	—	—	7.6	41.6	—	8.0	130.5	87.3	24.9	27.0
NGC2403	160.4	—	35.0	—	79.8	100.2	7.2	—	266.9	44.9	17.8	14.3
NGC3031	131.9:	—	—	83.6	—	—	—	—	232.0:	627.9	153.2:	179.0
NGC3077	313.2	—	43.0	—	185.2	161.3	37.0	—	1263.1	279.7	117.0	94.4
NGC4194	385.3	40.2	70.1	—	239.1	270.7	31.4	64.6:	1946.6	815.7	230.6	237.3
NGC4853	—	—	—	—	—	—	—	—	28.4	22.8	—	—
NGC4861	—	—	—	—	507.2	3596.1	61.9	—	2015.4	175.3:	72.7	50.0
MRK66	148.2	24.3	11.0	—	43.2	125.3	7.6	—	121.3	21.5	—	—
MRK477	234.8	98.8	48.9	32.3	103.4	1221.9	—	84.0	569.1	159.0	87.8	91.9
NGC5728	264.0	74.7	—	32.3	64.5	1175.6	—	98.6	830.5	740.5	14.1	23.4
UGC9560	334.5	28.0	50.7	—	144.6	598.4	15.3	—	529.4	44.1	52.5	43.4
NGC5860	15.4	—	—	—	26.8	17.1	9.7	—	296.7	145.1	23.7	23.1
UGCA410	104.6	32.2	21.5	—	80.2	530.0	6.2	—	324.4:	20.1	15.9	14.7
NGC5996	107.6	11.7	15.3	12.7	82.8	31.2	8.6	—	50.0	190.4	40.1	39.1
NGC6052	376.2	13.4:	39.6	—	122.7	247.2	—	21.6	565.0	84.6	113.7	87.3
NGC6090	153.6	—	42.0	—	123.7	84.2	23.6	10.6	675.3	305.1	81.7	61.4
NGC6217	108.1:	—	14.8	—	92.9	35.8	—	18.0	607.4	391.4	119.8	65.7
MRK499	62.0	—	—	—	16.9	60.3	3.2	—	117.4	27.2	21.3	7.7
NGC6764	185.6	—	18.3	0.8:	66.4	71.4	—	46.1	592.7	326.0	133.4	116.0
NGC7250	333.4	14.7	30.9	—	104.8	364.7	—	12.8	483.2	99.3	76.2	54.5
MRK309	—	—	—	—	13.6	8.9	—	—	101.9	68.7	16.4	—
NGC7673	446.6	38.2	22.1	—	109.8	260.0	23.8	8.2	608.0	136.9	95.4	79.5
NGC7714	951.1	—	196.9	—	539.9	894.4	81.5	48.7	2795.8	999.4	321.7	239.1
MRK542	3.8	—	—	—	17.1	15.9	—	—	88.9	38.7	7.3	6.9

NOTES.—Flux unit = 10^{-15} ergs cm^{-2} s^{-1}. Entries followed by a colon indicate that the line identification is highly uncertain.

TABLE 7

FLUXES OF UV AND LESS COMMON EMISSION LINES

Galaxy	Ly-a	C IV	He II	C III]	C II]	[Ne IV]	Mg II	[Ne V]	He II	[Ar III]	[O II]
IC1586	—	—	16.7	—	—	—	—	—	—	—	—
NGC262	406.1	98.6	55.0	29.4	—	—	—	—	—	—	—
MRK357	131.3	—	—	—	—	—	—	—	—	—	—
IC214	—	—	—	—	—	—	—	11.0	—	—	—
NGC1023	—	—	—	—	—	—	—	—	—	—	119.0
NGC1068	—	3955.8	1559.7	1781.2	493.3	854.7	732.4:	2757.2:	503.4	—	—
NGC1569	—	—	—	16.7:	—	—	—	62.4:	15.5:	44.8	—
NGC1614	—	—	—	19.1	—	—	—	—	—	—	—
NGC2403	—	—	7.8:	—	—	—	—	—	—	8.5	—
NGC3031	—	75.1	12.7:	98.8:	52.5:	—	106.0	—	—	—	—
NGC4194	—	—	—	—	21.8	—	—	—	—	—	—
NGC4853	21.5	—	—	—	—	—	—	27.0	—	—	—
NGC4861	—	—	—	249.3	—	—	—	—	—	—	—
MRK66	49.6	—	—	—	—	—	—	—	—	—	—
MRK477	736.3	211.0	40.1	58.4	41.7	199.3	96.8	56.2	—	—	—
NGC5728	80.5	96.6	61.5	12.8	—	5.2	8.9	—	—	—	—
UGCA410	—	—	—	13.4	—	—	—	—	—	—	—
NGC5996	—	—	—	19.8	—	—	—	—	—	—	—
NGC6052	—	—	28.1	—	41.9	13.0	—	—	—	44.7	—
NGC6090	—	—	—	—	—	—	—	—	—	—	15.4
NGC7250	—	—	—	—	13.1	—	—	—	—	37.3	—
MRK309	—	—	—	—	—	—	—	—	—	—	—
NGC7673	—	—	36.0:	—	19.6:	—	18.9	—	—	16.8	—
NGC7714	—	—	—	—	—	—	—	—	—	—	79.5

NOTES.—Flux unit = 10^{-15} ergs cm^{-2} s^{-1}. Entries followed by a colon indicate that the line identification is highly uncertain.

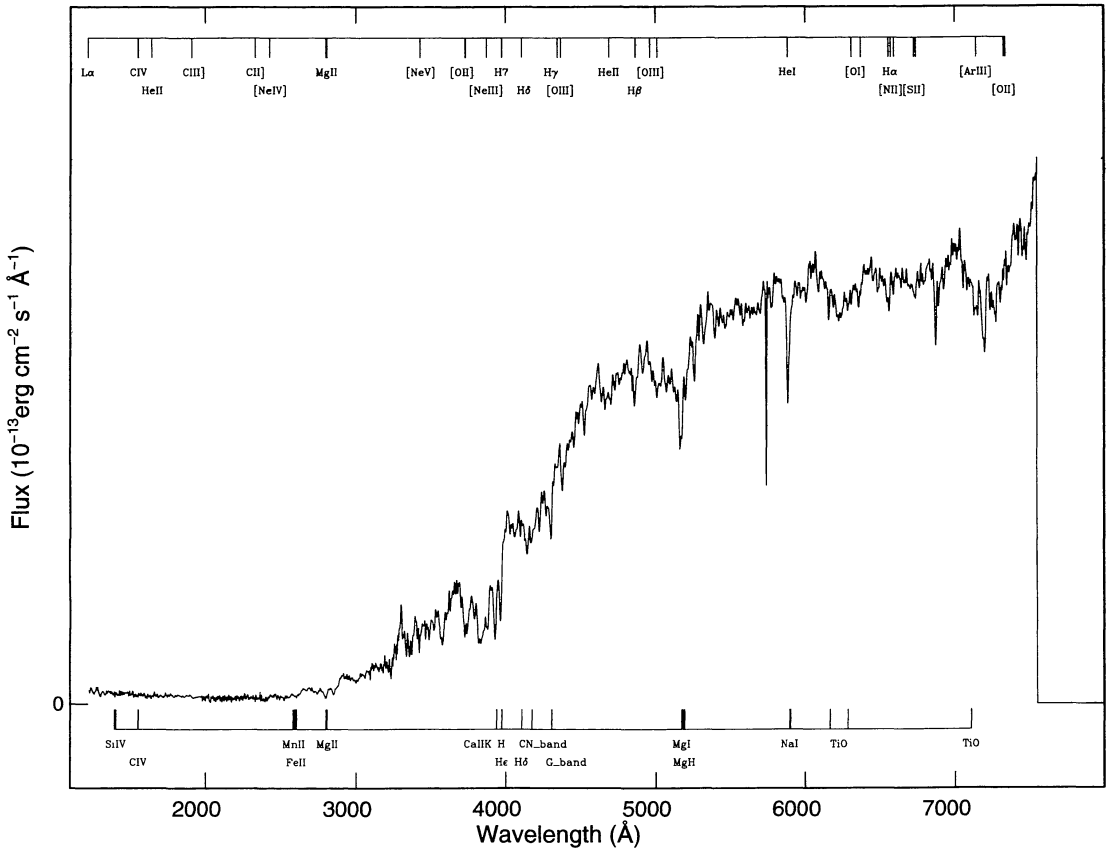

FIG. 1*a*

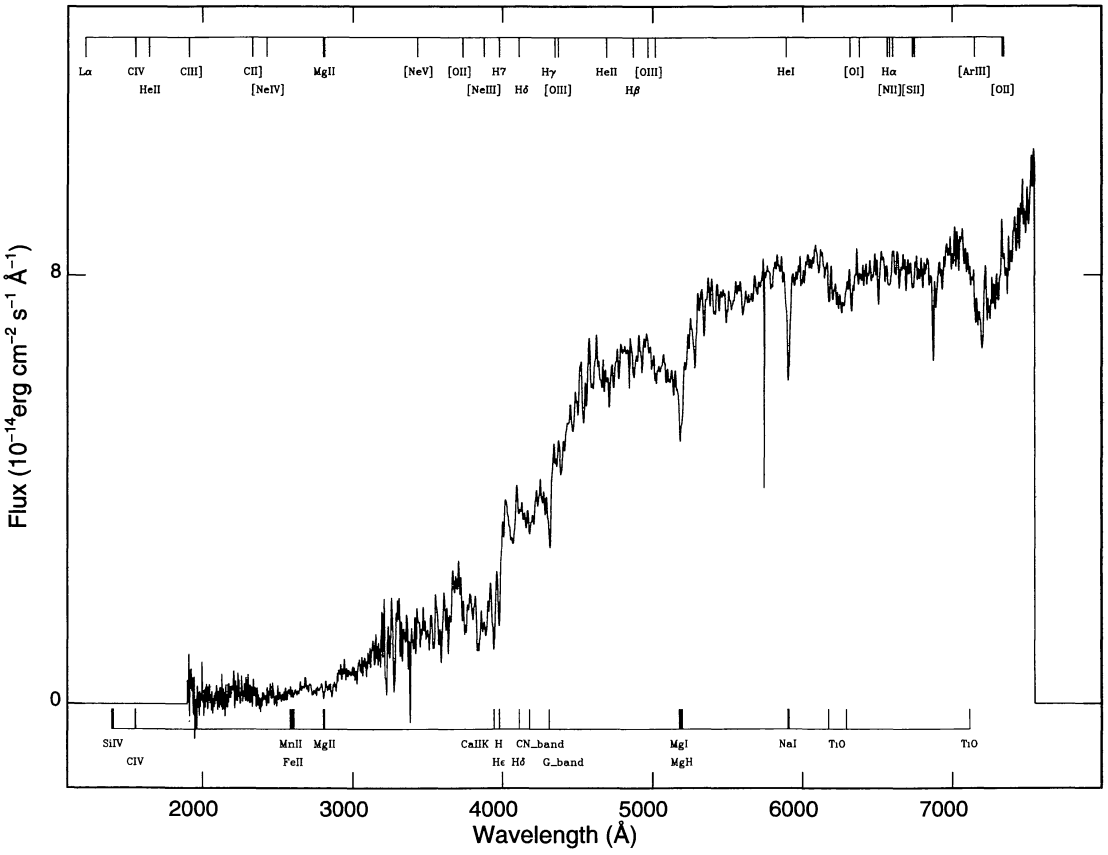

FIG. 1*b*

FIG. 1.—Normal galaxies (*a*) NGC 224 (bulge of Sb galaxy M31), (*b*) NGC 1023 (SB0), and (*c*) NGC 598 (Scd)

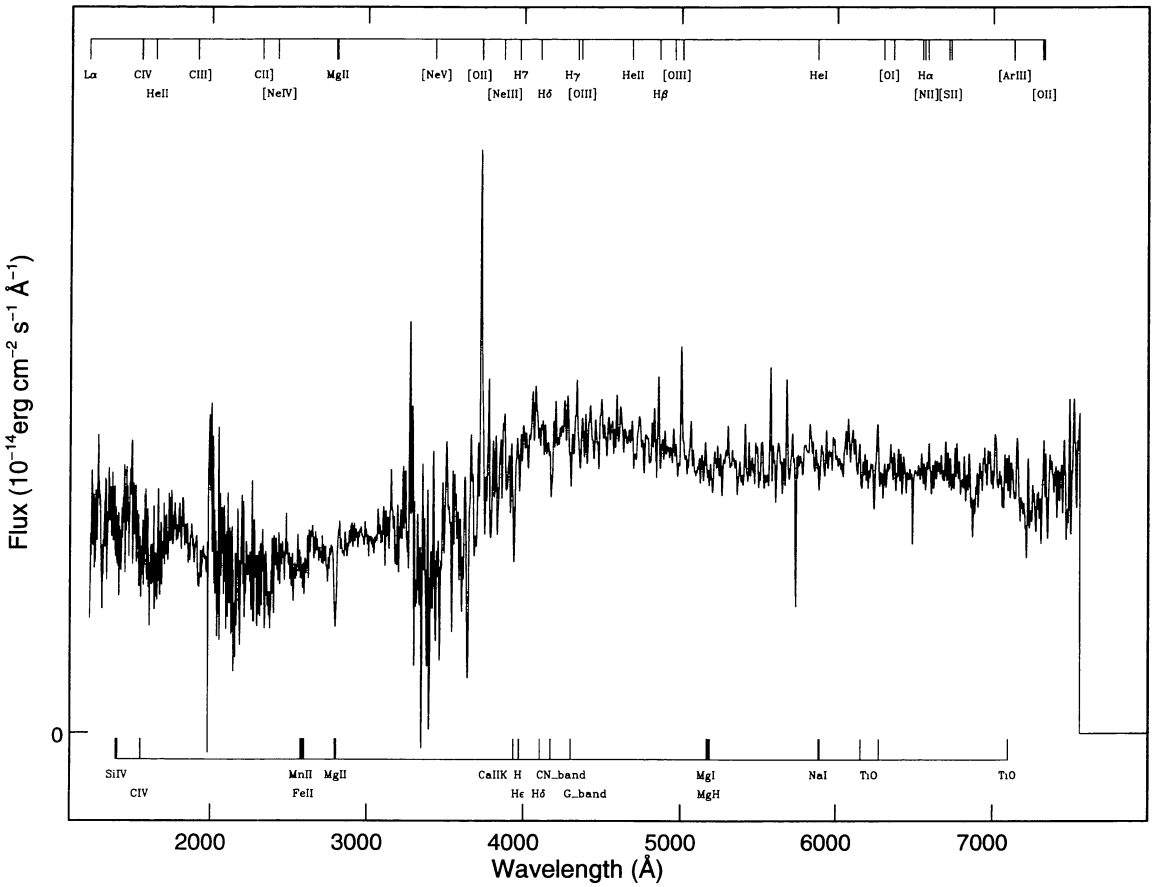

FIG. 1*c*

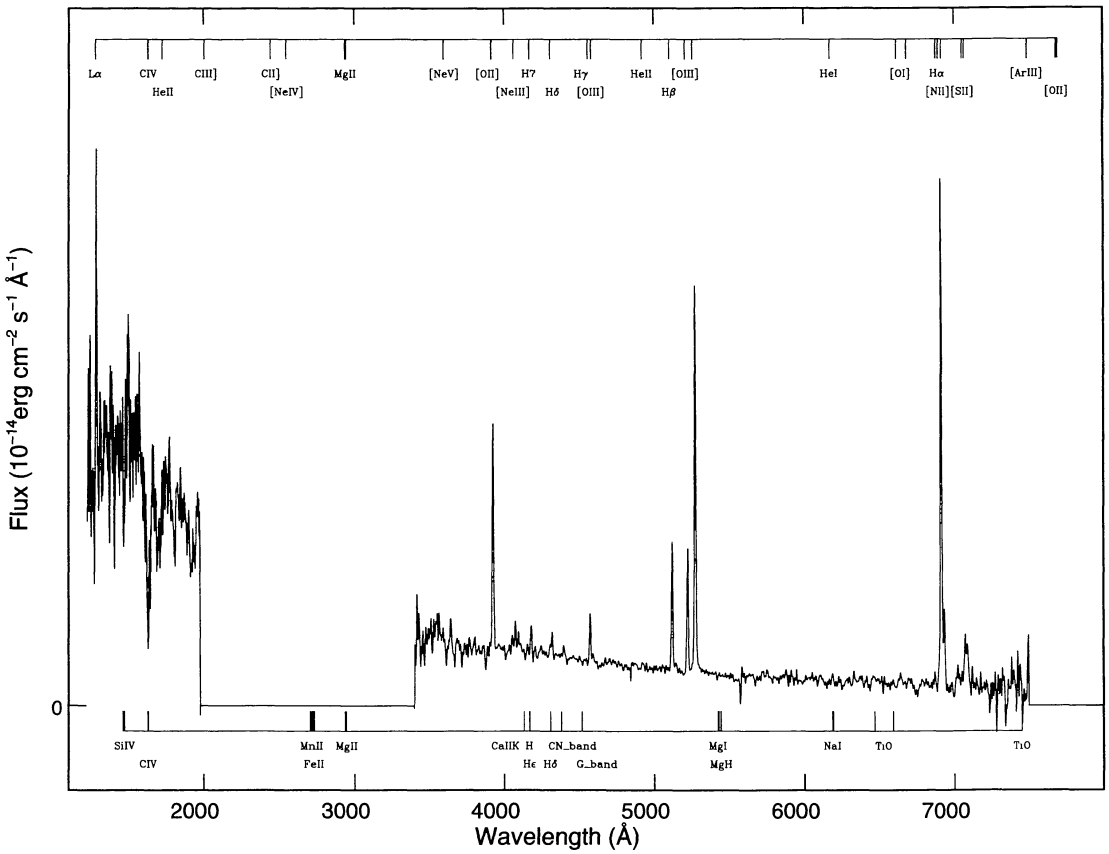

FIG. 2*a*

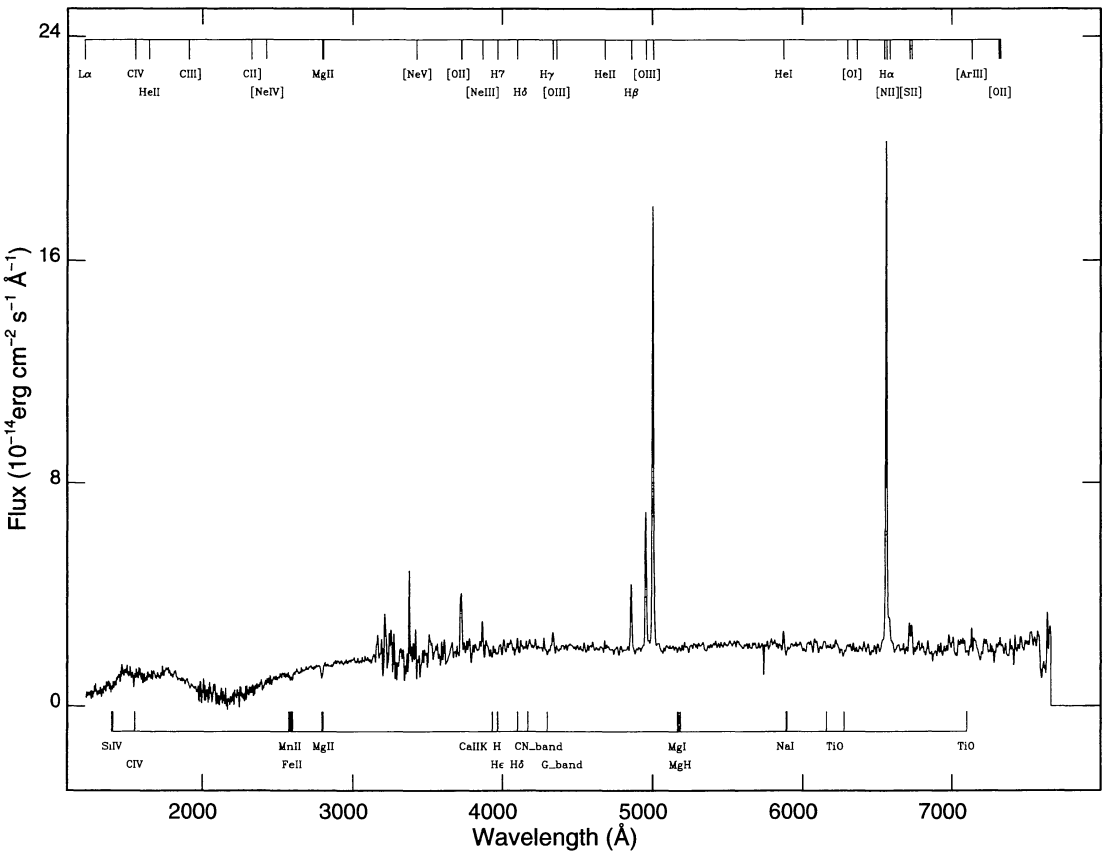

FIG. 2*b*

FIG. 2.—Starburst galaxies (*a*) Mrk 357, (*b*) NGC 1569, and (*c*) NGC 6052. Notice the extreme effects of Galactic reddening occurring in NGC 1569.

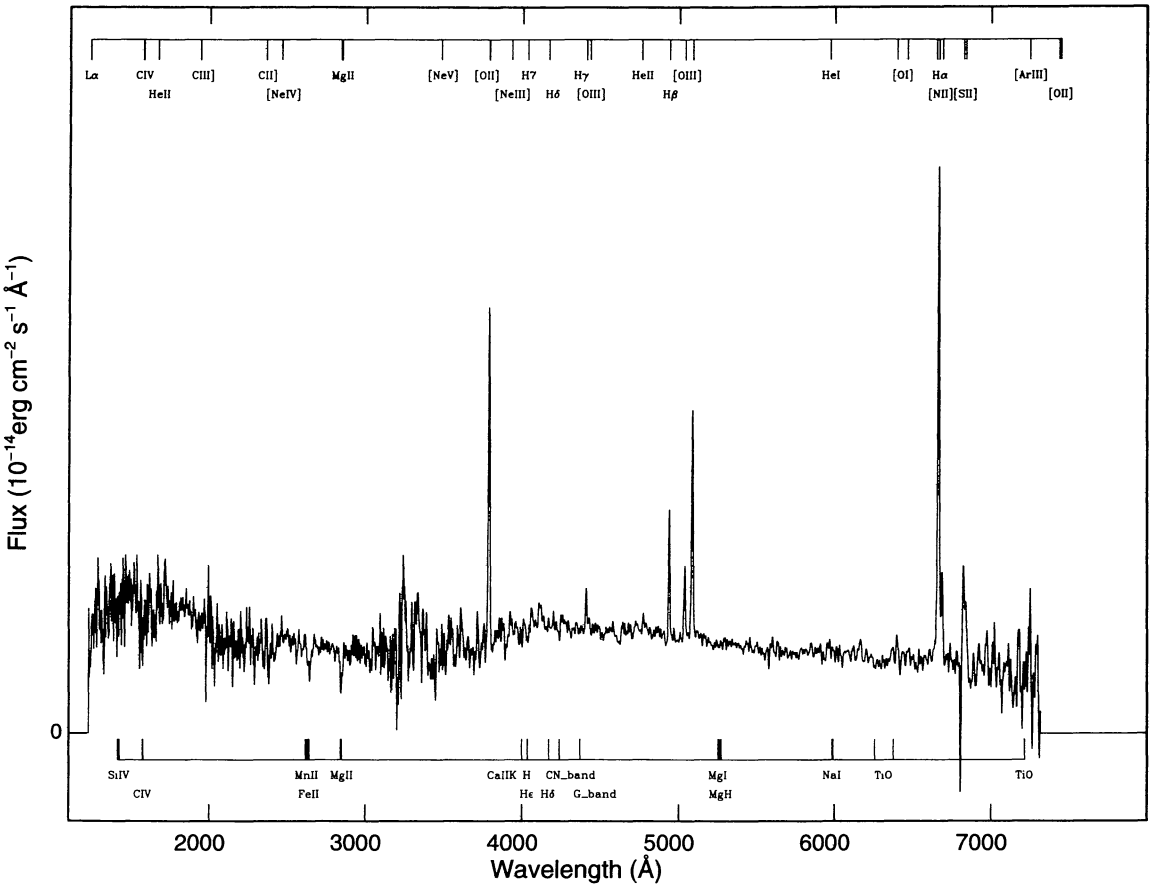

FIG. 2*c*

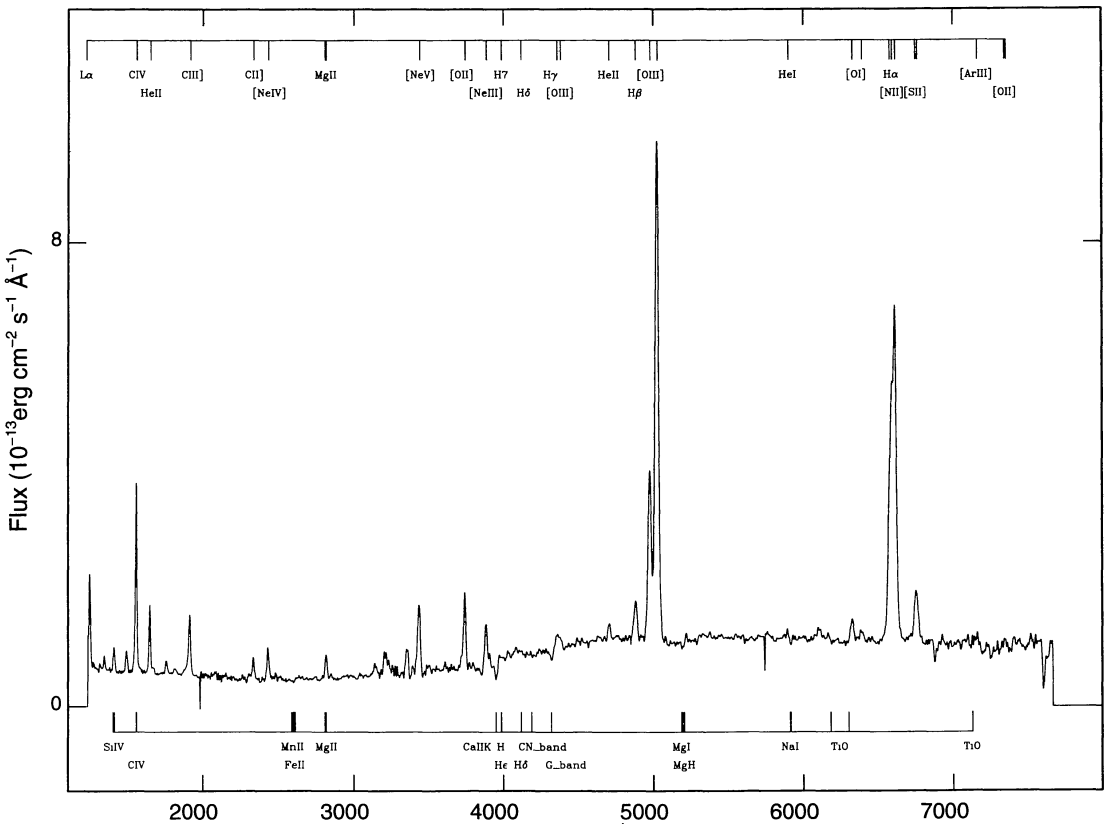

FIG. 3*a*

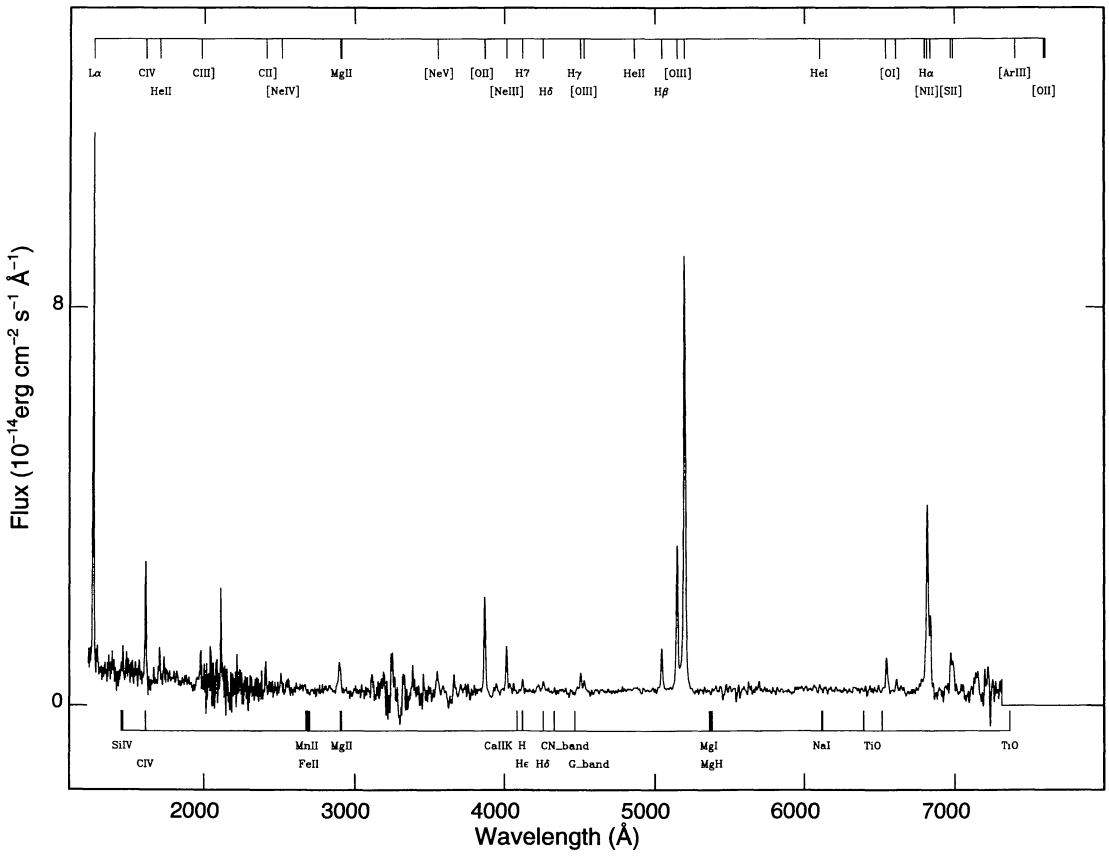

FIG. 3*b*

FIG. 3.—Seyfert 2 galaxies (*a*) NGC 1068 and (*b*) Mrk 477

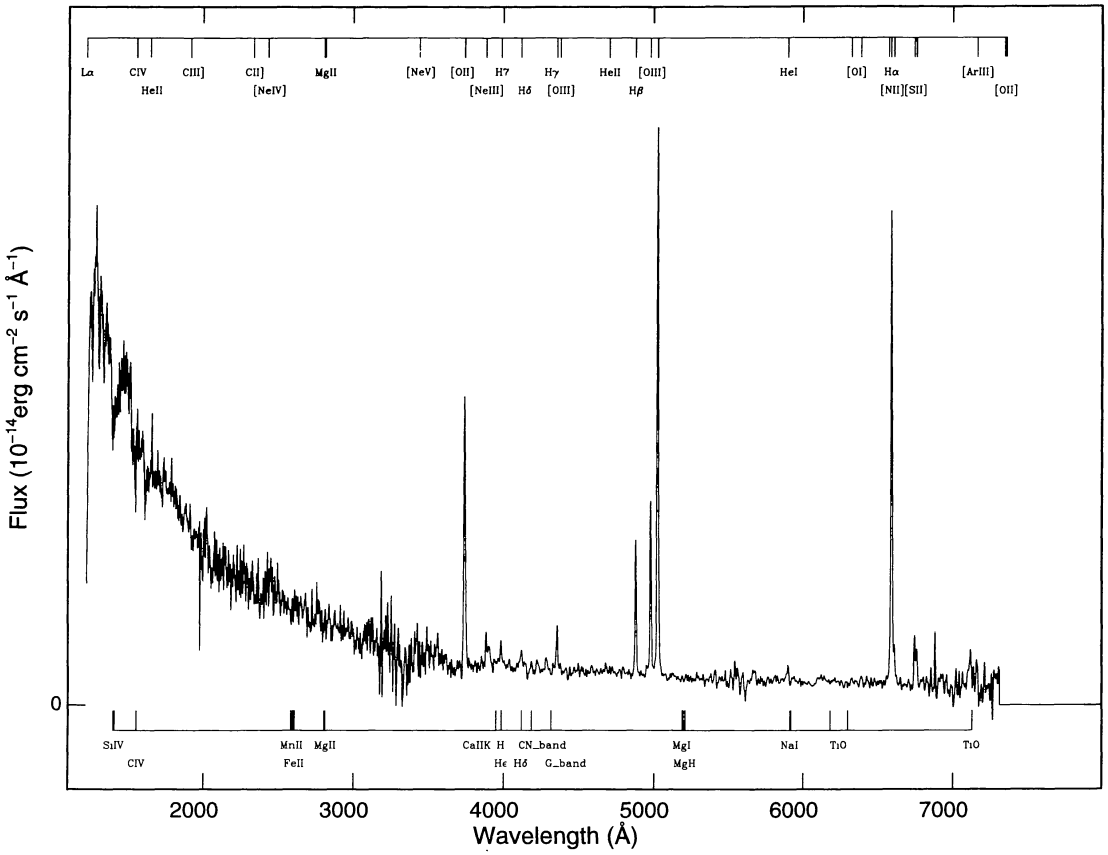

FIG. 4*a*

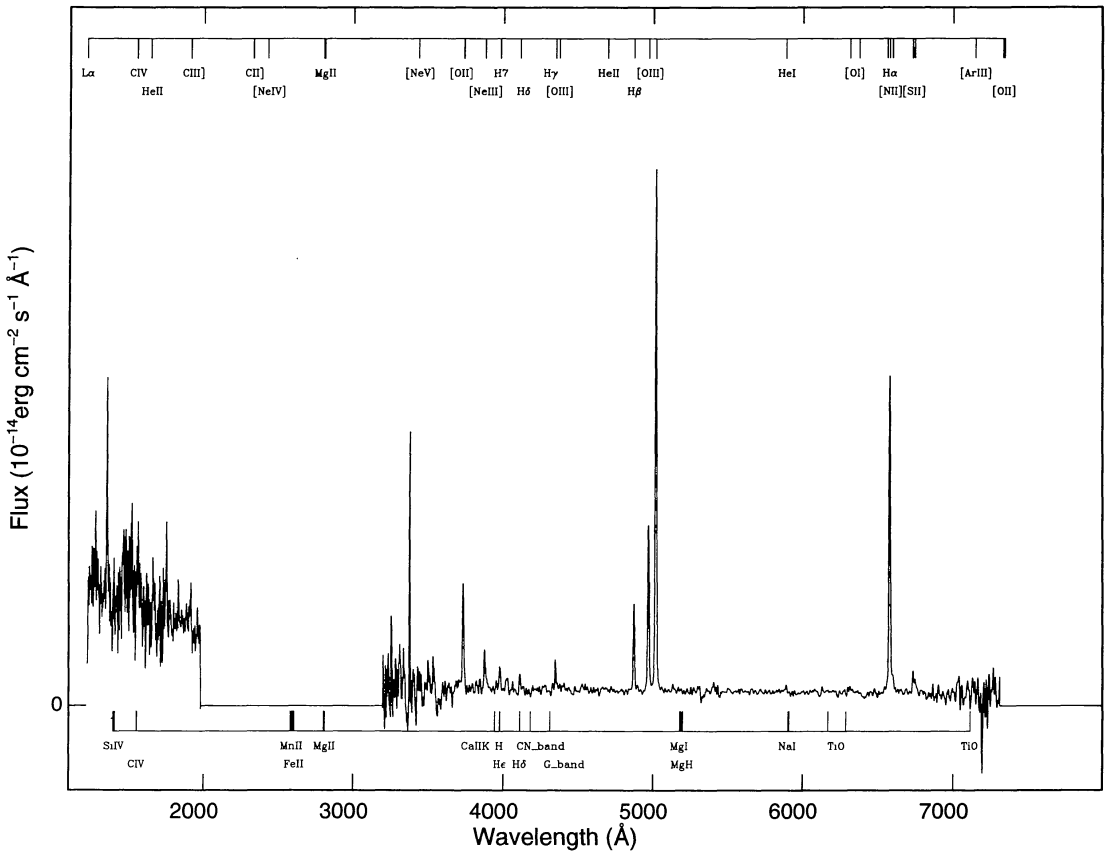

FIG. 4*b*

FIG. 4.—Blue compact dwarf galaxies (*a*) UGC 9560 and (*b*) UGCA 410

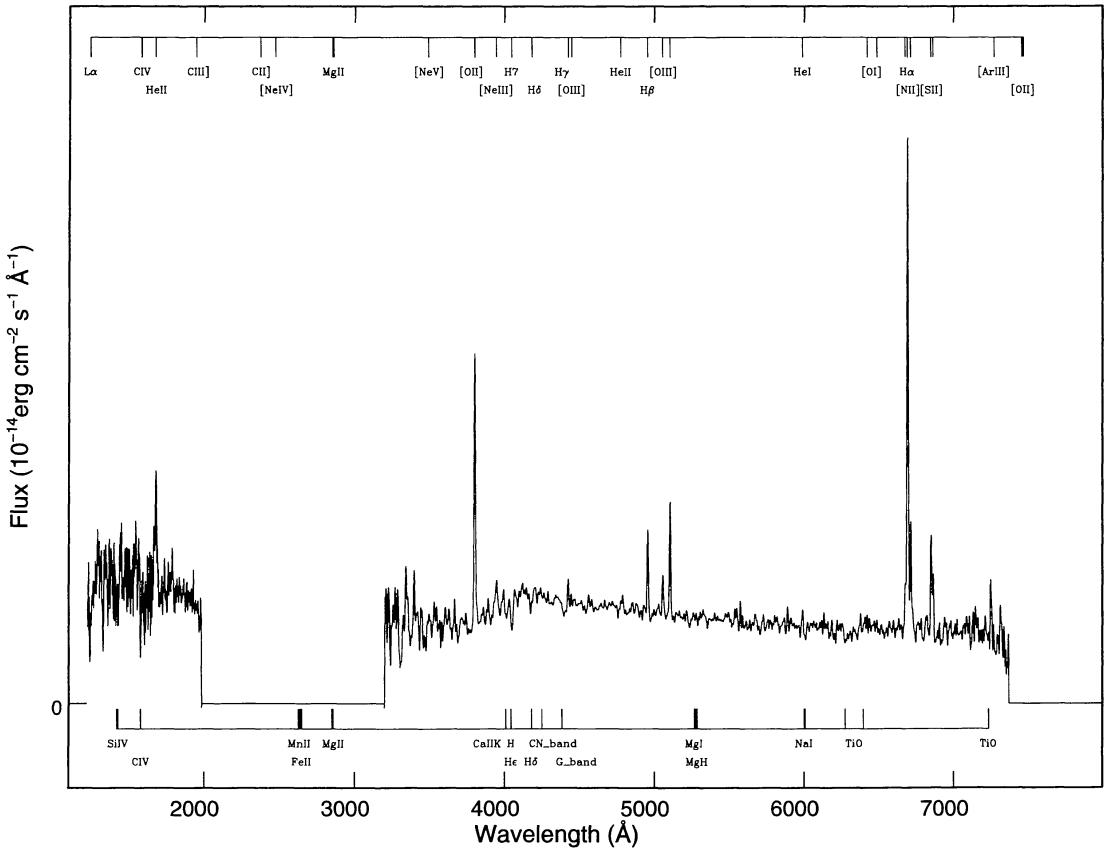

FIG. 5*a*

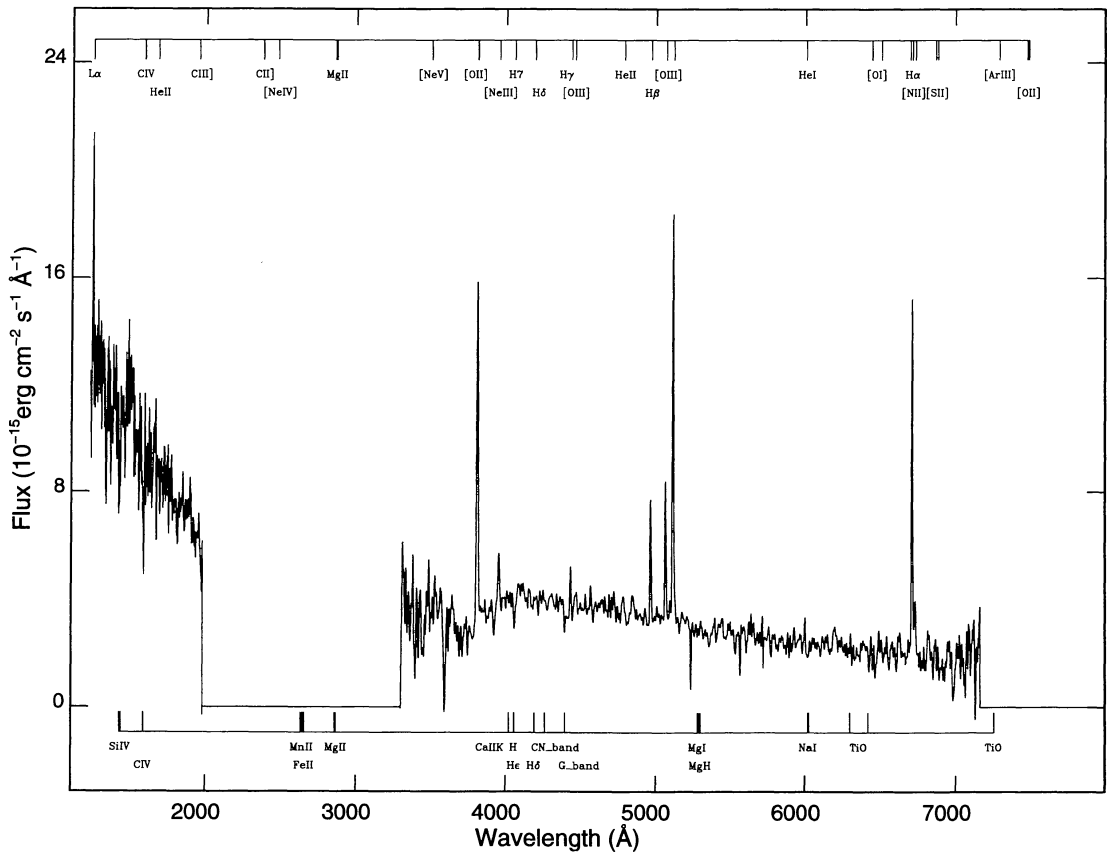

FIG. 5*b*

FIG. 5.—Blue compact galaxies (*a*) IC 1586 and (*b*) Mrk 66

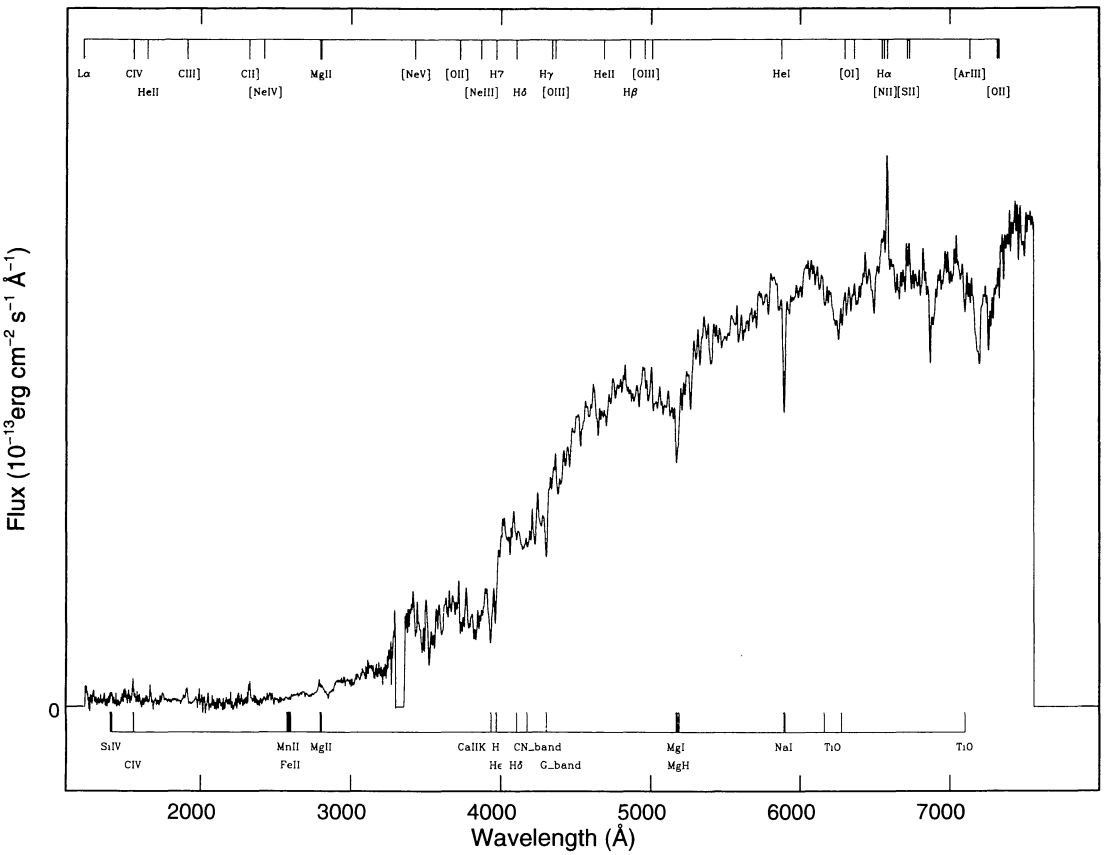

FIG. 6.—Liner galaxy NGC 3031

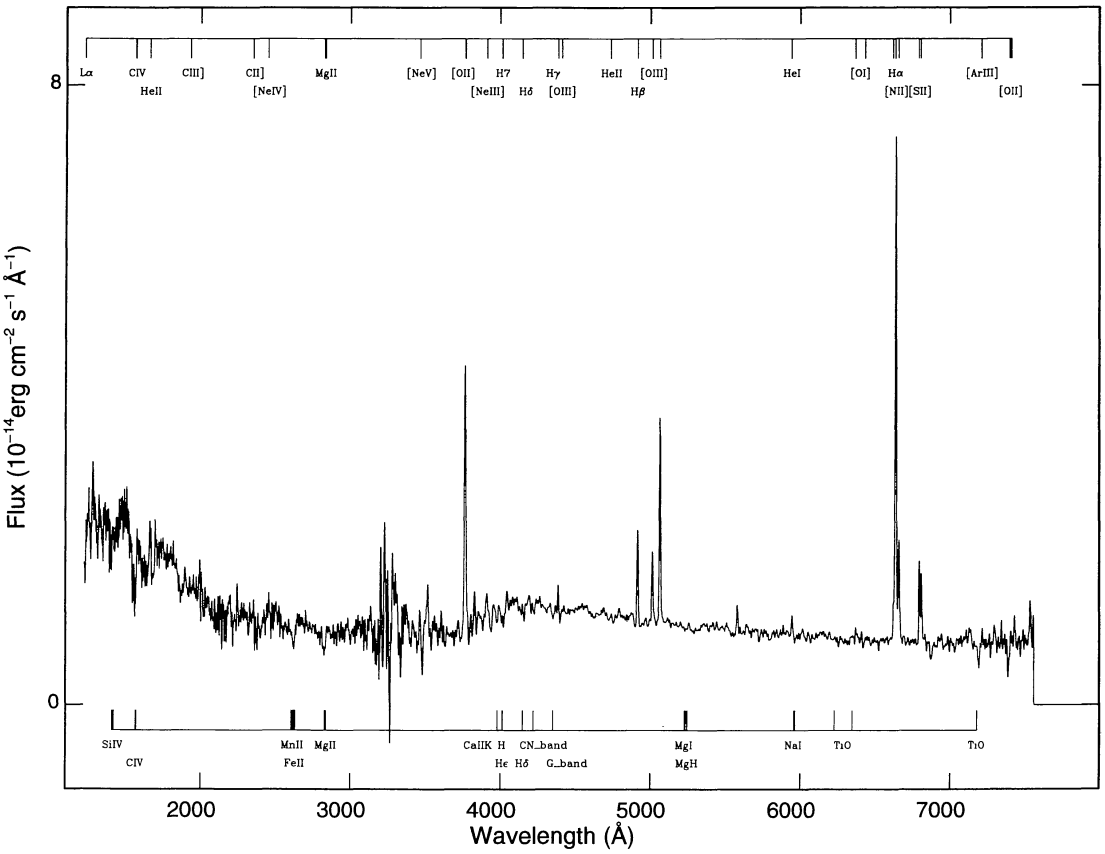

FIG. 7.—H II galaxy NGC 7673

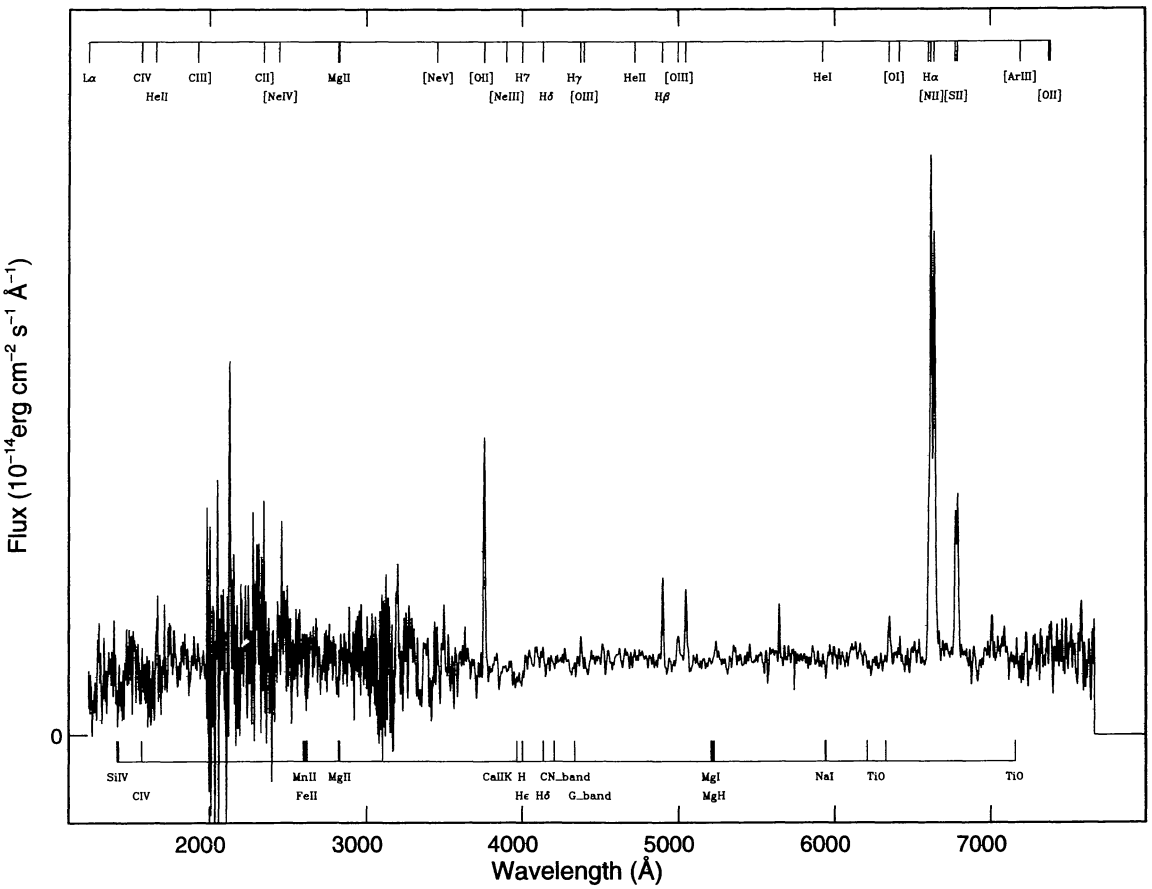

FIG. 8.—LINER–H II galaxy NGC 6764

TABLE 8

MEAN EMISSION-LINE RATIOS PER ACTIVITY CLASS

Activity Class	[O III]/Hβ	[N II]/Hα	[S II]/Hα	Hα/Hβ	L(Hα) (10^{40} ergs s^{-1})
Normal	1.625 ± 0.418 (3)	0.606 ± 0.432 (3)	0.144 ± 0.033 (2)	5.082 ± 2.457 (2)	3.2 ± 5.2 (3) 0.1–9.2
SB	2.356 ± 2.469 (13)	0.909 ± 1.340 (12)	0.316 ± 0.390 (13)	5.957 ± 3.183 (13)	102.9 ± 109.4 (13) 39.2–356.8
Sy2	17.998 ± 6.743 (5)	0.838 ± 0.431 (5)	0.333 ± 0.381 (5)	9.713 ± 6.713 (5)	137.1 ± 150.8 (5) 10.7–354.2
BCDG	8.027 ± 2.138 (3)	0.104 ± 0.018 (3)	0.112 ± 0.062 (3)	3.893 ± 0.204 (3)	80.9 ± 125.2 (3) 8.2–225.5
BCG	3.518 ± 1.538 (3)	0.276 ± 0.036 (3)	0.286 ± 0.054 (2)	5.222 ± 2.154 (3)	34.1 ± 7.7 (3) 25.7–71.7
LINER	...	3.627 (1)	1.432 (1)	...	0.1 (1)
LINER/H II	1.452 (1)	0.737 (1)	0.387 (1)	8.926 (1)	28.8 (1)
H II	3.197 (1)	0.302 (1)	0.288 (1)	5.537 (1)	52.2 (1)

NOTE.—The number in parentheses following the line ratio indicates the number of galaxies contributing to the mean.

and has a central burst of star formation, the difference in aperture size is most likely the cause of the difference in continuum shape. The increased aperture size allows for a much greater contribution from older population stars.

Our spectrum of NGC 6217 shows a redder optical spectrum than in Kennicutt. Again, Kennicutt's aperture is much larger than ours (90″ circular versus 13″.5 circular). NGC 6217 is classified as an SBbc galaxy (Kinney et al. 1993). The larger aperture size allows for more of the galaxy's arms to be included in the spectrum. Thus the bluer spectrum of Kennicutt could be reflecting the contribution of star-forming regions in the spiral arms.

5.2. *Emission-Line Features*

Table 8 contains the mean emission-line ratios for select emission lines in each activity class. We have excluded NGC 4194 from our sample of blue compact galaxies because of the large effects of extinction which skew our values (Calzetti, Kinney, & Storchi-Bergmann 1994). All other galaxies are included for the comparisons.

TABLE 9

MEAN CONTINUUM COLORS PER ACTIVITY CLASS

Activity Class	$C(14-35)$	$C(40-53)$
Normal	0.570 ± 1.057 (4)	0.104 ± 0.589 (5)
SB	−0.604 ± 0.828 (13)	−0.065 ± 0.216 (13)
Sy2	0.099 ± 0.986 (5)	0.464 ± 0.342 (5)
BCDG	−2.114 ± 0.029 (2)	−0.312 ± 0.221 (2)
BCG	−0.868 ± 0.338 (3)	−0.232 ± 0.127 (3)
LINER	2.684 (1)	4.173 (1)
LINER/H II	0.052 (1)	0.024 (1)
H II	−0.985 (1)	−0.031 (1)

NOTE.—The numbers in parentheses reflect the number of galaxies contributing to the mean value.

The [O III]/Hβ ratio contains the flux in both oxygen lines at λλ4959, 5007. Likewise, [N II]/Hα contains the flux in both [N II] lines at λλ6548, 6583. We have measured the stronger line of each pair, then calculated the strength of the weaker line based on the recombination relations given by McCall, Rybski, & Shields (1985):

$$[\mathrm{O\ III}](4959) = 0.35[\mathrm{O\ III}](5007)$$

$$[\mathrm{N\ II}](6548) = 0.34[\mathrm{N\ II}](6583).$$

In the case of [S II]/Hα, the contributions of both the lines at λλ6717,6731 were measured.

Seyfert 2's have the largest ratios, which is in agreement with the results presented in Storchi-Bergmann et al. (1994). The [O III]/Hβ ratio decreases steadily through the BCDG, BCG, SB, and normal classes (leaving out those classes for which there were only one measurement taken). The [N II]/Hα and [S II]/Hα ratios show no clear trend, but the dispersion is quite large for our measurements.

The final column in Table 8 contains the mean Hα luminosity (as well as the range in values) for each activity class. This value was derived (on the extinction-corrected spectra) from the apparent (B_T) and absolute (M_B) magnitudes from Kinney et al. (1993, Table 1). The Seyfert 2's and SB galaxies are by far the most luminous in Hα, followed by the BCDG, H II, BCG, and LINER/H II classes. The normal and LINER samples show little Hα luminosity.

5.3. *Continuum Colors*

We also present the continuum colors $C(14-35)$ and $C(40-53)$, as defined in Table 9 of Storchi-Bergmann, Calzetti, & Kinney (1994):

1995ApJS...97..331M

TABLE 10

MEAN REST WAVELENGTH EQUIVALENT WIDTHS OF ABSORPTION FEATURES PER ACTIVITY CLASS

Activity Class	Si IV	C IV	Fe II	Mg II	Ca K	Ca	CN	G Band	Mg	Na I
Normal	4.1 ± 1.7 (5)	8.2 ± 7.5 (4)	3.0 ± 2.9 (5)	5.8 ± 3.2 (5)	4.5 ± 2.8 (6)	4.6 ± 2.8 (6)	1.8 ± 0.6 (4)	3.2 ± 1.1 (5)	2.5 ± 1.9 (6)	2.5 ± 2.3 (5)
SB	5.9 ± 3.6 (13)	7.9 ± 2.8 (12)	5.1 ± 1.4 (6)	5.2 ± 2.0 (6)	2.4 ± 1.7 (11)	3.1 ± 2.4 (12)	1.8 ± 1.3 (9)	1.0 ± 0.8 (10)	1.2 ± 0.7 (13)	1.8 ± 0.9 (11)
Sy2	1.2 ± 0.6 (2)	7.5 (1)	3.2 ± 2.7 (3)	...	6.4 ± 2.9 (5)	3.6 ± 1.8 (3)	2.4 ± 1.4 (4)	4.2 ± 1.4 (5)	2.6 ± 1.0 (5)	2.2 ± 1.2 (5)
BCDG	3.0 ± 1.0 (3)	3.1 ± 1.5 (3)	1.0 ± 0.4 (2)	3.2 (1)	1.8 ± 0.1 (2)	...	1.6 (1)	4.4 ± 3.7 (2)	0.8 (1)	1.4 ± 1.2 (3)
BCG	4.9 ± 1.3 (3)	7.7 ± 2.1 (3)	...	...	1.4 ± 1.4 (2)	4.8 ± 1.0 (3)	1.3 ± 0.7 (3)	1.9 ± 1.4 (3)	1.0 ± 0.7 (3)	2.6 ± 0.9 (3)
LINER	...	...	2.0: (1)	...	8.6 (1)	4.9 (1)	...	4. 5 (1)	4.2 (1)	4.0 (1)
LINER/H II	8.7 (1)	5.7: (1)	8.2: (1)	6.3 (1)	7.7 (1)	5.9 (1)	0.4: (1)	1.7 (1)	...	2.5 (1)
H II	3.0 (1)	9.0 (1)	5.8 (1)	5.6 (1)	0.1: (1)	3.4: (1)	1.7: (1)	1.3: (1)	0.2: (1)	0.1: (1)

NOTE.—The number in parentheses following each equivalent width indicates the number of galaxies contributing to the mean.

$$C(14-35) = -2.5 \log \frac{F_{\lambda 1355}}{F_{\lambda 3500}}$$

$$C(40-53) = -2.5 \log \frac{F_{\lambda 4020}}{F_{\lambda 5313}}.$$

Our colors generally agree with the trends presented in Storchi-Bergmann et al. (1995). The BCDGs are the bluest sample, followed by H II, BCG, SB, LINER–H II, Sy2, normal, to LINER, with our one LINER (NGC 3031) being significantly redder than the rest of the classes.

5.4. *Absorption Features*

Table 10 contains the mean rest wavelength equivalent widths of the absorption features for each activity class. Because of the low signal-to-noise ratio of our data, it is difficult to draw any conclusions from these data.

The authors thank Pete Challis, Christine Schwartz, and Cindy Taylor for help with observing and data reduction. The authors acknowledge support from the NASA grants NAG5-1143, NAG5-1675, NAG5-2498, NAG5-3757, and from the STScI Directors Research Fund.

This research has made use of the NASA/IPAC Extragalactic Database (NED) which is operated by the Jet Propulsion Laboratory, Caltech, under contract with the et Propulsion Laboratory, Caltech, under contract with the National Aeronautics and Space Administration.

REFERENCES

Bica, E. 1988, A&A, 195, 76
Calzetti, D., Kinney, A. L., & Storchi-Bergmann, T. 1994, ApJ, 430
Kennicutt, R. C. 1992a, ApJ, 388, 310
———. 1992b, ApJS, 79, 255
Kinney, A. L., Bohlin, R. C., Calzetti, D., Panagia, N., & Wyse, R. F. G. 1993, ApJS, 86, 5
McCall, M. L., Rybski, P. M., & Shields, G. A. 1985, ApJS, 57, 1
Robert, C., Leitherer, C., & Heckman, T. M. 1993, ApJ, 418, 749
Storchi-Bergmann, T., Calzetti, D., & Kinney, A. L. 1994, ApJ, 429, 572
Storchi-Bergmann, T., Kinney, A. L., & Challis, P. 1995, ApJS, in press